Extensive molecular mapping of TCRα/δ- and TCRβ-involved chromosomal translocations reveals distinct mechanisms of oncogene activation in T-ALL

Sandrine Le Noir,[1] Raouf Ben Abdelali,[1] Marc Lelorch,[2] Julie Bergeron,[1] Stephanie Sungalee,[3] Dominique Payet-Bornet,[3] Patrick Villarèse,[1] Arnaud Petit,[4] Céline Callens,[1] Ludovic Lhermitte,[1] Laurence Baranger,[5] Isabelle Radford-Weiss,[2] Marie-José Grégoire,[6] Hervé Dombret,[7] Norbert Ifrah,[8] Salvatore Spicuglia,[9] Serge Romana,[2] Jean Soulier,[10] Bertrand Nadel,[3] Elizabeth Macintyre,[1] and Vahid Asnafi[1]

[1]Université Paris 5 Descartes, Centre National de la Recherche Scientifique (CNRS) UMR 8147, and Department of Hematology, Assistance Publique–Hôpitaux de Paris (AP-HP), Hôpital Necker-Enfants Malades, Paris, France; [2]Université Paris 5 Descartes, Department of Cytogenetics, AP-HP, Hôpital Necker-Enfants Malades, Paris, France; [3]Centre d'Immunologie de Marseille-Luminy (Inserm U631), CNRS, Unité Mixte de Recherche 6102, Université de la Méditerranée, Marseille, France; [4]Department of Hematology, AP-HP Hôpital Armand Trousseau, Paris, France; [5]Department of Hematology, Centre Hospitalier, Angers, France; [6]Laboratoire de Génétique, Centre Hospitalier Universitaire (CHU) de Nancy-Brabois, Vandoeuvre-Les-Nancy, France; [7]University Paris 7, Hôpital Saint-Louis, AP-HP, Department of Hematology and Institut Universitaire d'Hématologie, Équipe d'Accueil 3518, Paris, France; [8]Pôle de Recherche et d'Enseignement Supérieur Les Universités Nantes Angers le Mans, CHU Angers service des Maladies du Sang et Inserm U892, Angers, France; [9]Technological Advances for Genomics and Clinics, Inserm U1090, Marseille, France; and [10]Inserm U728, Institut Universitaire d'Hematologie, Hopital Saint-Louis, Universite Paris VII Denis Diderot, Faculte de Medecine, Paris, France

Chromosomal translocations involving the *TCR* loci represent one of the most recurrent oncogenic hallmarks of T-cell acute lymphoblastic leukemia (T-ALL) and are generally believed to result from illegitimate V(D)J recombination events. However, molecular characterization and evaluation of the extent of recombinase involvement at the TCR-oncogene junction has not been fully evaluated. In the present study, screening for TCRβ and TCRα/δ translocations by FISH and ligation-mediated PCR in 280 T-ALLs allowed the identification of 4 previously unreported TCR-translocated oncogene partners: *GNAG*, *LEF1*, *NKX2-4*, and *IL2RB*. Molecular mapping of genomic junctions from *TCR* translocations showed that the majority of oncogenic partner breakpoints are not recombinase mediated and that the regulatory elements predominantly used to drive oncogene expression differ markedly in *TCR*β (which are exclusively enhancer driven) and *TCR*α/δ (which use an enhancer-independent cryptic internal promoter) translocations. Our data also imply that oncogene activation takes place at a very immature stage of thymic development, when Dδ2-Dδ3/Dδ3-Jδ1 and Dβ-Jβ rearrangements occur, whereas the bulk leukemic maturation arrest occurs at a much later (cortical) stage. These observations have implications for T-ALL therapy, because the preleukemic early thymic clonogenic population needs to be eradicated and its disappearance monitored. (*Blood*. 2012;120(16):3298-3309)

Introduction

T-cell acute lymphoblastic leukemias (T-ALLs) are malignant proliferations of T-cell precursors arrested at various stages of development.[1,2] Our understanding of T-ALL oncogenesis has advanced rapidly over the past decade, and numerous combinations of multigenic aberrations and oncogenic synergy have been identified.[3] Among these, chromosomal translocations involving the *TCR* loci represent the recurrent oncogenic hallmark of T-ALL.[4] *TCR* translocations predominantly involve the *TCR*α/δ locus at chromosome 14q11 or *TCR*β at chromosome 7q34, but rearrangement of *TCR*γ at chromosome 7p15 is virtually unrecognized.[4] Such translocations are generally believed to result from illegitimate V(D)J recombination events and to lead to ectopic activation of oncogenes because of their the potent positive regulatory elements of the *TCR* locus or loss of the negative regulatory element.[5,6] Specific mechanistic differences in V(D)J-mediated translocation mechanisms have been shown to guide break location and clustering in T-ALL.[7] Two main types of oncogenic translocations involving the *TCR*β and *TCR*α/δ have been described.[8] In the so-called type 1 translocations (supplemental Figure 1, available on the *Blood* Web site; see the Supplemental Materials link at the top of the online article), a cryptic but functional recombination signal sequence (cRSS) is present near the oncogene and is mistakenly targeted by the RAG recombinase as a partner for a recombining *TCR* gene segment. Translocations of this type consequently cluster (within tens of base pairs) at this cryptic site. In type 2 translocations, only the *Ig/TCR* locus breaks are generated by RAG targeting, and the translocation results from repair mistakes between *TCR*-rearranging intermediates and DNA breaks in the vicinity of the oncogene. One distinctive feature of the 2 mechanisms is that the former involves DNA transactions between 2 breaks (4 DNA ends), both of which are thought to be recombinase mediated, whereas the latter involves DNA transactions between 3 breaks (6 DNA ends), with only the *TCR* breaks being due to recombinase activity. In T-ALL, the basis for DNA breakage at the other breakpoint is largely unknown, probably heterogeneous, and not necessarily specific to lymphoid malignancies. It

Submitted April 20, 2012; accepted July 31, 2012. Prepublished online as *Blood* First Edition paper, September 4, 2012; DOI 10.1182/blood-2012-04-425488.

The online version of this article contains a data supplement.

The publication costs of this article were defrayed in part by page charge payment. Therefore, and solely to indicate this fact, this article is hereby marked "advertisement" in accordance with 18 USC section 1734.

is generally considered that both the *TCR* locus and the partner oncogene need to be in an accessible chromatin configuration to undergo translocation. Because *TCR* rearrangements occur sequentially in a highly coordinated fashion during both normal and leukemic T-lymphoid development, molecular characterization of *TCR* translocations can throw light on the timing of the oncogenic event.

In humans, the earliest T-cell precursor was defined as $CD34^+/CD7^+/CD45RA^+/sCD3^-/CD2^-/CD5^-/CD1a^-$.[9] Progressive lineage restriction and acquisition of T-cell potential after migration from the BM to the thymus is likely to involve successive differentiation into $CD5^+CD1a^-$ T/NK precursors, followed by definitive T-cell commitment of $CD34^+sCD3^-CD4/8$ double-negative (DN) thymocytes at the $CD5^+CD1a^+$ developmental stage.[10] This is followed by appearance of intermediate single positivity for CD4 immediately before the transition to the CD4/8 double-positive (DP) cell stage. *TCR*δ rearrangement initiates within the thymus, at the $CD5^+CD1a^-$ T/NK stage; *TCR*γ and *TCR*β rearrangements initiate at the $CD1a^+$ stage, before the start of cTCRβ expression; and β selection during the $CD34^+CD1a^+ \rightarrow$ intermediate single positivity transition.[10] *TCR*δ rearrangement first involves V-D or D-D junctions, which may then proceed to D-J or VD-J complete junctions, possibly (or unless) followed by *TCR*δ locus deletion because of V-Jα recombination in αβT-lineage–committed precursors.[11] T-ALLs reproduce the normal stages of thymic cell development, notably with respect to the succession of *TCR* rearrangements.[12]

Several significant T-ALL oncogenes, including *TLX1* (10q24), *HOXA* (7p15), *LMO2* (11p13), *LMO1* (11p15), *TAL1* (1p32), and *NOTCH1* (9q34), were identified from TCR chromosomal translocation analysis.[13,14] A recent, but unique, FISH study demonstrated that TCR-oncogene translocations detected karyotypically are largely underestimated, notably those involving *TCRβ,* which were detected in 19% of 126 T-ALLs.[4] The *TCR* partner oncogene was not identified in several cases. Similarly, molecular characterization and evaluation of the extent of recombinase involvement at the TCR-oncogene junction has not been fully evaluated in T-ALL. We have recently shown that some oncogenes can influence the type of *TCR*δ rearrangements that have leukemogenic potential, because TLX1 overexpression inhibits the TCRα enhanceosome and therefore leads to auto-extinction of *TCR-TLX1* translocated cells, in which the TCRα enhancer is on the same chromosome as *TLX1*.[15]

In the present study, we searched for *TCR*β and *TCR*α/δ translocations by FISH and ligation-mediated PCR (LM-PCR) in 280 T-ALL patients and characterized their molecular junctions. We confirm the high incidence of *TCR*β translocations in both adult and pediatric T-ALL patients and have identified 4 unreported TCR oncogene partners. We also show that the majority of oncogene partner breakpoints are not recombinase mediated and that the regulatory elements predominantly used to drive oncogene expression differ in *TCR*β (which are exclusively enhancer driven) and *TCR*α/δ (which use an enhancer-independent cryptic internal promoter) translocations

Methods

T-ALL samples

Diagnostic samples from a consecutive series of 280 T-ALL patients, 128 pediatric and 152 adults (16 years or over), were screened for TCRβ and TCRα/δ rearrangement by FISH and/or LM-PCR. Sample collection and analyses were obtained with informed consent in accordance with the Declaration of Helsinki with approval from the institutional review boards of institutions that participated in this study. Diagnosis of T-ALL was based on the World Health Organization 2008 criteria, defined by expression of cytoplasmic and/or surface CD3, and negativity of CD19 and MPO, as described previously.[1] The only criterion for inclusion in the study was the availability of appropriate material for cytogenetic/molecular analysis. Immunophenotyping, molecular marker identification of *STIL-TAL1* (also known as *SIL-TAL1*) and *PICALM-MLLT10* (also known as *CALM-AF10*) fusion transcripts, oncogene quantification (TLX1, TLX3, LMO1, LMO2, TAL1, and HOXA9), and TCR immunogenotyping were performed as described previously.[1,16]

Cytogenetic and FISH analysis

Cytogenetic analysis with R-banding was performed at various institutions on metaphases from BM aspirates taken at diagnosis using standard procedures. Karyotypes were described according to the International System for Human Cytogenetic Nomenclature (ISCN), 2005.

Screening by FISH for *TCR*β and *TCR*δ rearrangements was performed at Necker Hospital (Hôpital Necker-Enfants Malades, Paris, France). We designed a dual-color probe using RP11-114L10 and RP11-1084E14 BAC clones for TCRβ and CTD-2552B11 and RP11-1083M21 for TCRα/δ. For the *GNAQ* translocation, we used 3 probes spanning the *GNAQ*, *TLX1*, and TCRα/δ loci: BAC clones RP11-959B21, RP11-98I1, RP11-951C10, RP11-624L13 labeled with streptavidin cyanine 5 for the *GNAQ* locus; RP11-31L23, RP11-119018, RP11-324L3, RP11-179B2, RP11-1031N22 labeled with rhodamine-dUTP for *TLX1*; RP11-137H15 and CTD-2552B11 labeled with FITC-dUTP (Vysis) for *TCR*α/δ. For the *TCR*α/δ-*NKX2.4* translocation, *TCR*α/δ probes were coupled with CTD-2338F9 and CTD-322103. For the *TCR*β-*LEF1* and *TCR*β-*IL2RB* translocations, *TCR*β probes were associated, respectively, with RP11-32K24, RP11-45D5, RP11-1123B16 and RP11-349I23, and with RP11-191N10 and RP11-643I13. For the remaining loci, we used RP11-1065L8 and RP11-782G4 (*LMO1*), RP11-1008P23 and RP11-1018M13 (*LMO2*), RP11-159M21 and RP11-1112E24 (*TAL1*), and RP11-1136C8 and 1132K14 (*HOXA*).

LM-PCR and sequencing

LM-PCR assays were performed as described previously.[17,18] Briefly, 330 ng of genomic DNA was digested using a combination of 6 blunt-end restriction enzymes (*Dra*I, *Pvu*II, *Stu*I, *Sma*I, *Ssp*I, and *Eco*RV). For the TCRβ-based LM-PCR rounds, ligation of 50 pmol of an adaptor to both ends of the restriction fragments was followed by 2 rounds of PCR using nested adaptor-specific (AP1 and AP2) oligonucleotide primers, as well as Dβ1, Dβ2, Jβ1.6, and Jβ2.7 oligonucleotide primers. The LM-PCR products were sequenced in both directions using the specific primer and the nested adaptor-specific primer (AP2). The sequences were blasted to the National Center for Biotechnology Information (NCBI) nucleotide database (http://www.ncbi.nlm.nih.gov/BLAST) and the Ensembl genome browser (http://www.ensembl.org/Multi/blastview). Junctions identified by LM-PCR were validated with a specific primer set flanking the identified breakpoint.

Quantitative RT-PCR

We used a TaqMan assay to quantify HOXA9, LMO2, and TAL1 transcripts with the following primers: HOXA9F: 5′GAAAACAATGCTGAGAATGAGAGC3′, HOXA9 Probe: Fam-ACAAGCCCCCCATCGATCCCA-Tamra, HOXA9R: 5′CGCGCATGAAGCCAGTT3′, TAL1F: 5′ACAATCGAGTGAAGAGGAGACCTTC, TAL1 Probe: Fam-CTATGAGATGGAGATGGAGATTACTGATTG-Tamra, TAL1R: 5′ACGCCGCACAACTTTGGT 3′, LMO2F: 5′GCCATCGAAAGGAAGAGCCT3′, LMO2 probe: Fam-CCTGCTGACATGCGGCGGCT-Tamra, LMO2R: 5′AAGTAGCGGTCCCCGATGTT3′ 40 cycles were run on ABI 7500HT (Applied Biosystems) as described previously.[17] NKX2-4 was quantified with kit hs01380224-g1 (Applied Biosystems).

Extrachromosomal recombination assay

As described previously,[19] a recombination plasmid (supplemental Figure 7A) in which the 2 sequences to be tested for V(D)J recombination are

separated by a termination signal was constructed. The approximately 0.8-kb sequence located immediately 5′ of *TLX1* and containing the breakpoint "hot spot" (5′ *TLX1* sequence), and the germline-recombining Dδ3 segment flanked by its 2 consensus RSS were inserted upstream to the chloramphenicol acetyltransferase gene (CAT). Two 5′ *TLX1* sequences were tested: the SR16 sequence covers nucleotides −794 to +15 relative to the position of the first ATG of *TLX1*'s first exon and the SR17 construct is shorter and covers position −794 to −227.

The recombination plasmid and expression plasmids for RAG1, RAG2, and TdT were cotransfected into eukaryotic NIH3T3 fibroblasts according to the manufacturer's instructions (FuGENE HD Transfection Reagent; Roche Applied Science). After Dpn1 digestion and purification, the plasmids were transfected in Top10 *E coli* bacteria (Invitrogen) and plated on ampicillin (100 μg/mL)/chloramphenicol (15 μg/mL). After 16-18 hours of incubation, the ampicillin/chloramphenicol–selected colonies were probed by direct PCR (Taq; Invitrogen) with core plasmid primers (p5b or P6b and Vect3c) flanking the inserted recombination construction. The PCR products were then sequenced and analyzed individually.

Results

TCRβ translocation screening and oncogene partner identification in adult and pediatric T-ALL patients

*TCR*β locus translocations were identified by FISH in 40 of 280 (14%) T-ALL patients. The *TCR*β translocation frequency was comparable in adult (24 of 152; 16%) and pediatric (16 of 128, 12.5%) patients. Only 12 of 28 *TCR*β-translocated T-ALL patients with an available karyotype harbored a 7q34 abnormality, confirming the low rate of classic karyotypic informativity for this category of translocation (Table 1).

LM-PCR and/or dual-color FISH identified the oncogene partners from 37 of the 40 *TCR*β-split T-ALLs (Table 1). No partner could be identified in only 3 cases. As expected, a high frequency of homeodomain oncogene deregulation was observed (25 of 40; 63%), including 13 *TCR*β-*HOXA* and 12 *TCR*β-*TLX1* translocations. Of the 13 *TCR*β-*HOXA* patients, 11 had material available for HOXA transcript quantification; all demonstrated HOXA9 overexpression (median HOXA9/ABL: 277%, range, 54%-3562%). Similarly, all 12 patients with *TCR*β-*TLX1* translocations demonstrated high-level TLX1 overexpression (data not shown). Contrary to TLX1$^+$ T-ALLs, which demonstrate a virtually uniform early cortical stage of αβ-lineage maturation arrest,[16,20] *TCR*β-*HOXA* translocations showed a predominantly mature TCR expressing the γδ-lineage phenotype (7 of 13 TCRγδ$^+$), especially in adult T-ALL patients. Two TCRγδ–expressing T-ALL patients demonstrated HOXA activation both by *TCR*β-*HOXA* translocation and PICALM-MLLT10 fusion transcript (Table 1). Among previously reported *TCR*β oncogene partners, 2 *LMO1*, 3 *LMO2*, 3 *MYB*, and 1 *TAL1* TCRβ-translocated cases were identified, confirming the low frequency of these translocations in T-ALL.

Two new *TCR*β partners were identified by LM-PCR: *LEF1* (lymphoid enhancer factor 1) on chromosome 4q25 and *ILR2B* (IL-2 receptor beta chain) on chromosome 22q13. The *TCR*β-*LEF1*–translocated case was a cortical CD1a$^+$/pre-αβ adult T-ALL patient (T-ALL439 in Table 1; this patient also demonstrated a novel *TCR*α/δ-*NKX2-4* translocation, see next paragraph). LM-PCR analysis identified the breakpoints within intron 3 of *LEF1* (Figure 1A). Interestingly, this *TCR*β-*LEF1* translocation leads to the LEF1 transcript inactivation, because RT-PCR analysis of the full-length LEF1 transcript (exons 1-11) demonstrated that the wild-type full-length *LEF1* transcript was not detectable (supplemental Figure 2A) and SNP-6 CGH-array analysis of this case confirmed that the nontranslocated *LEF1* allele harbored partial intragenic deletion (supplemental Figure 2B). These data are consistent with the reported tumor-suppressor function of LEF1 in T-cell oncogenesis.[21] The case of *TCR*β-*IL2RB*–translocated T-ALL was a cortical CD1a$^+$/pre-αβ pediatric patient with a normal karyotype (number 17 in Table 1). Molecular breakpoint mapping revealed that the translocation put the *ILR2B* gene under the control of the TCRβ enhancer (Eβ; Figure 1B).

TCRα/δ translocation screening and oncogene partner identification in adult and pediatric T-ALL patients

Of 280 T-ALL patients, 38 (13%) demonstrated a *TCR*α/δ translocation by cytogenetic and FISH analysis. These were more frequent in adult patients (29 of 152; 19%) compared with pediatric patients (9 of 128; 7%; $P = .002$). As for the *TCR*β–translocated patients, only 15 of 30 *TCR*α/δ–translocated T-ALL patients with available karyotypic data harbored 14q11 abnormalities (Table 2).

LM-PCR and/or dual-color FISH allowed the identification of 36 oncogene partners from these 38 split-*TCR*α/δ T-ALL patients (Table 2), with only 2 cases remaining unidentified. *TLX1* represented the most frequent *TCR*α/δ partner (as expected, mainly in adults [19 of 29] compared with 2 of 9 in children), but there were also 7 cases of *LMO2*, 5 *TAL1*, and 1 *MYC*, with no apparent age influence. Compared with the relatively frequency of *TCR*β-*HOXA*, there was a striking absence of *TCR*α/δ-*HOXA* rearrangements. One trans-rearrangement between the TCRδ and IgH loci was observed in a TLX3-expressing T-ALL patient (Table 2).

Two new partners were identified by LM-PCR: *NKX2-4* (NK2 homeobox 4) on chromosome 20p11 and *GNAQ* (guanine nucleoside binding protein) on chromosome 9q21. Molecular junctional characterization of the *TCRα/δ-NKX2-4* (T-ALL439) demonstrated that the translocation put the *NKX2-4* gene under the control of the TCRα enhancer (Eα; Figure 1C). Quantitative RT-PCR analysis of NKX2-4 transcript expression confirmed NKX2-4 overexpression in this sample compared with other T-ALL, peripheral blood lymphocytes, and thymic samples (supplemental Figure 3). The *TCR*α/δ-*GNAQ-TLX1* patient (T-ALL244 in Figure 1D and Table 2) demonstrated a karyotypic t(9;10;14)(q22;q23;q11). On the basis of LM-PCR results and the overexpression of *TLX1*, we performed 3-color FISH analysis using a combination of TLX1 (red), GNAQ (yellow), and TCRα/δ (green) probes. We demonstrated a fusion of *GNAQ* and *TCR*α/δ, *GNAQ* and *TLX1*, on the der(9) and der(10), respectively. However, FISH analysis on the der(14) revealed a complex rearrangement and a fusion on 14q, of, sequentially, *TLX1*, *GNAQ*, and *TCR*α/δ (telomere to centromere). By LM-PCR it was possible to identify the *GNAQ-TCR*α/δ junction (Figure 1D), but not the *TLX1* junction(s).

Another patient (T-ALL500) showed a translocation with 3 partners, including *TLX1*, *TCR*δ, and *TCR*β, which was confirmed by 3-color FISH analysis (supplemental Figure 4).

TCR translocations occur more frequently in early cortical, IMβ/pre-αβ T-ALLs and show patterns of oncogenic synergy

TCR translocations, especially those involving *TCR*α/δ, occurred more frequently within T-ALL patients with the early-cortical, IMβ/pre-αβ phenotype (Tables 1 and 2). However, these translocations are observed at all stages of maturation arrest, including mature TCRγδ- and TCRαβ–expressing T-ALLs, but are relatively rare in immature cases (Table 3). Among the recognized oncogenic groups in T-ALL, patterns of "cooperative" oncogenes can be

Table 1. Biological characteristics of T-ALL with TCRβ-oncogene translocation

T-ALL UPN	Age, y	Phenotype	Oncogenetic	TCRβ partner	Karyotype
Pediatric T-ALL (n = 16)					
282	15	IMβ	Negative	HOXA	46,XY[23]
246	11	IMβ	Negative	HOXA	ND
8	7	Pre-αβ	Negative	HOXA	46,XX[50]
284*	10	TCRγδ$^+$	Negative	HOXA	46,XY,t(10;13)(q?;q?)[3]/46,XY[2]
290†	2	IMβ	Negative	MYB	46,XY,t(6;7)(q?23;q?)[19]/46,XY[3]
247†	2	IMγ	Negative	MYB	46,XX,t(6;7)(q?22;q35),t(8;14)(q22;q11),del(11)(q22)[14]/46,XX[1]
280‡	14	IMβ	TLX1	TLX1	46,XX,t(9;9)(q10;q10)[12]
336‡	12	IMβ	TLX1	TLX1	47,XX,del(9)(p12),+del(9)(p12)[9]/46,XX[5]
316‡	11	Pre-αβ	TLX1	TLX1	46–48,XY,inv(1)(p2?p3?),−4,−9,−9,−11,del(11)(q2?),del(12)(p?),−18,+5−7mar [cp17]/46,XY[3]
17	3	Pre-αβ	STIL-TAL1	IL2RB	46,XY[25]
374	12	TCRαβ$^+$	Negative	LMO2	46,XX[20]
75	10	TCRαβ$^+$	Negative	LMO2	46 XY,del(6)(q15q23)[1]/46,XY[38]
270	13	Pre-αβ	Negative	TAL1	47,XY,t(1;7)(p22;q32),−6,+8,del(9)(q13q21),add(17)(p?13),r(?6)[8]/46,XY[14]
346‡	5	IMβ	TLX1	TCRβ	ND
328†	1	Pre-αβ	Negative	MYB	46,XY,t(6;7)(q23;q35)[16]/46,XY[6]
308	10	IM0	Negative	Unknown	47,XY,+19[6]/46,XY[5]
Adult T-ALL (n = 24)					
174	21	IM0	Negative	HOXA	46,XY,del(6)(p12p22),inv(14)(q22q31),add(20)(q11)[7]/46,XY,idem,add(8)(q24)[10]/46,XY[5]
366	28	Pre-αβ	Negative	HOXA	46,XY[20]
368	64	TCRαβ$^+$	Negative	HOXA	ND
183	24	TCRγδ$^+$	Negative	HOXA	46,XY[20]
181	29	TCRγδ$^+$	Negative	HOXA	47,XY,+11[7]/47,XY,+21[4]/46,XY[1]
536	44	TCRγδ$^+$	Negative	HOXA	46,XY[20]
347	16	TCRγδ$^+$	Negative	HOXA	46,XY[26]
232	45	TCRγδ$^+$	PICALM-MLLT10	HOXA	ND
264	38	TCRγδ$^+$	PICALM-MLLT10	HOXA	46,XX,del(7)(p?),add(5)(q?)[9]
43‡	36	IMγ	TLX1	TLX1	46,XY[20]
546‡	28	IMβ	TLX1	TLX1	46,XY,add(4)(p?12),del(6)(q12),t(7;10)(q34;q24)[7]/46,XY[9]
474‡	32	Pre-αβ	TLX1	TLX1	46,XY,t(7;10)(q34;q24)[30]
57‡	35	Pre-αβ	TLX1	TLX1	46,XX[20]
84‡	17	Pre-αβ	TLX1	TLX1	46,XY,t(7;10)(q35;q24)[9]/46,XY,?t(5;18)(p11;p11)[3]/46,XY[3]
547‡	20	Pre-αβ	TLX1	TLX1	46,XY,t(7;10)(q34;q24)[15]/46,idem,del(6)(q2?1q2?6)[2]/46,XY[3]
500‡	26	Pre-αβ	TLX1	TCRδ and TLX1	46,XY[20]
28‡	47	Pre-αβ	TLX1	TLX1	46,XX[50]
379‡	58	Pre-αβ	TLX1	TLX1	46,XX,t(7;10)(q35;q24)[13]
234‡	16	IMβ	Negative	LMO1	46,XY,dup(2)(q11q37),?del(6)(p22)[15]
380	38	Pre-αβ	STIL-TAL1	LMO1	46.XX,add(9)(p?)[18]/46,XX[5]
178	26	Pre-αβ	Negative	LMO2	46,XY,t(7;11)(q35;p13)[16]/46,XY[1]
439	25	Pre-αβ	Negative	LEF-1	46,XY,t(4;7)(q2?5;q35),t(14;20)(q11;p1?2)[19]
497	19	Pre-αβ	Negative	Unknown	46,XY,t(7;9)(q34;q31),add(9)(q34)[18]
233	22	IMβ	TLX3	Unknown	48,XY,del(6)(q13q22),r(7),+8,+12[16]

Applying a TCR-based classification[1]: immature (IM) cases (surface and cytoplasmic TCRβ$^-$) comprised IM0, IMδ, and IMγ subtypes (harboring, respectively, a germline configuration of all three TCRβ, TCRδ, and TCRγ loci, only a TCRδ rearrangement, or in addition TCRγ-rearranged locus, accompanied or not by an incompletely rearranged DJβ locus); IMβ/pre-αβ cases included IMβ and pre-αβ subtypes (displaying VβDJβ rearrangement and, respectively, either a cTCRβ$^-$ or sTCR$^-$/cTCRβ+ phenotype); TCRαβ and TCRγδ cases harbored a cell surface TCRαβ or TCRγδ . *PICALM-MLLT10* and *STIL-TAL1* fusion transcripts were detected using RT-PCR as described previously.[1] *TLX1* and *TLX3* were detected using RQ-PCR as described previously.[16]

Negative indicates cases with neither *PICALM-MLLT10* and *STIL-TAL1* fusion transcripts nor *TLX1/TLX3* overexpression; ND, not done; and unknown, LM-PCR failures.

*Also reported in Soulier et al.[40]

†Also reported in Clappier et al.[41]

‡Also reported in Dadi et al.[15]

identified. PICALM-MLLTF10$^+$ T-ALLs lead to overexpression of HOXA but also coexist with *TCR*β-*HOXA* (this study) or *TCR*α/δ-*HOXA*,[22] as if the *PICALM-MLLT10* (also known as *CALM-AF10*)–induced HOXA expression left the locus accessible to DNA damage and subsequent translocation. Similarly, in patients with *STIL-TAL1* (also known as *SIL-TAL1*), TCR translocations mainly involve oncoproteins known for their collaboration with *TAL1* (*LMO1* and *LMO2*). Approximately 60% of translocation partner oncogenes belong to the superfamily of homeotic proteins, but there are striking differences in TCR involvement, in which *HOXA* is mostly translocated to *TCR*β, *TLX1* to both, and *TLX3* to neither, although *TLX3* is frequently deregulated by promoter substitution, particularly in pediatric T-ALL patients. No significant relation was observed with *NOTCH1/FBXW7* somatic mutations and *TCR*α/δ or *TCR*β translocations, although TCR translocations altogether tended to be more frequent in *NOTCH1/FBXW7*–mutated patients ($P = .04$), probably because they are preferentially arrested at a cortical IMβ/pre-αβ stage (Table 3).

TCR-oncogene translocations precede the predominant stage of leukemic maturation arrest

LM-PCR analysis identified 20 and 24 molecular junctions from *TCR*β-translocated patients (Figure 2 and supplemental Figure 5)

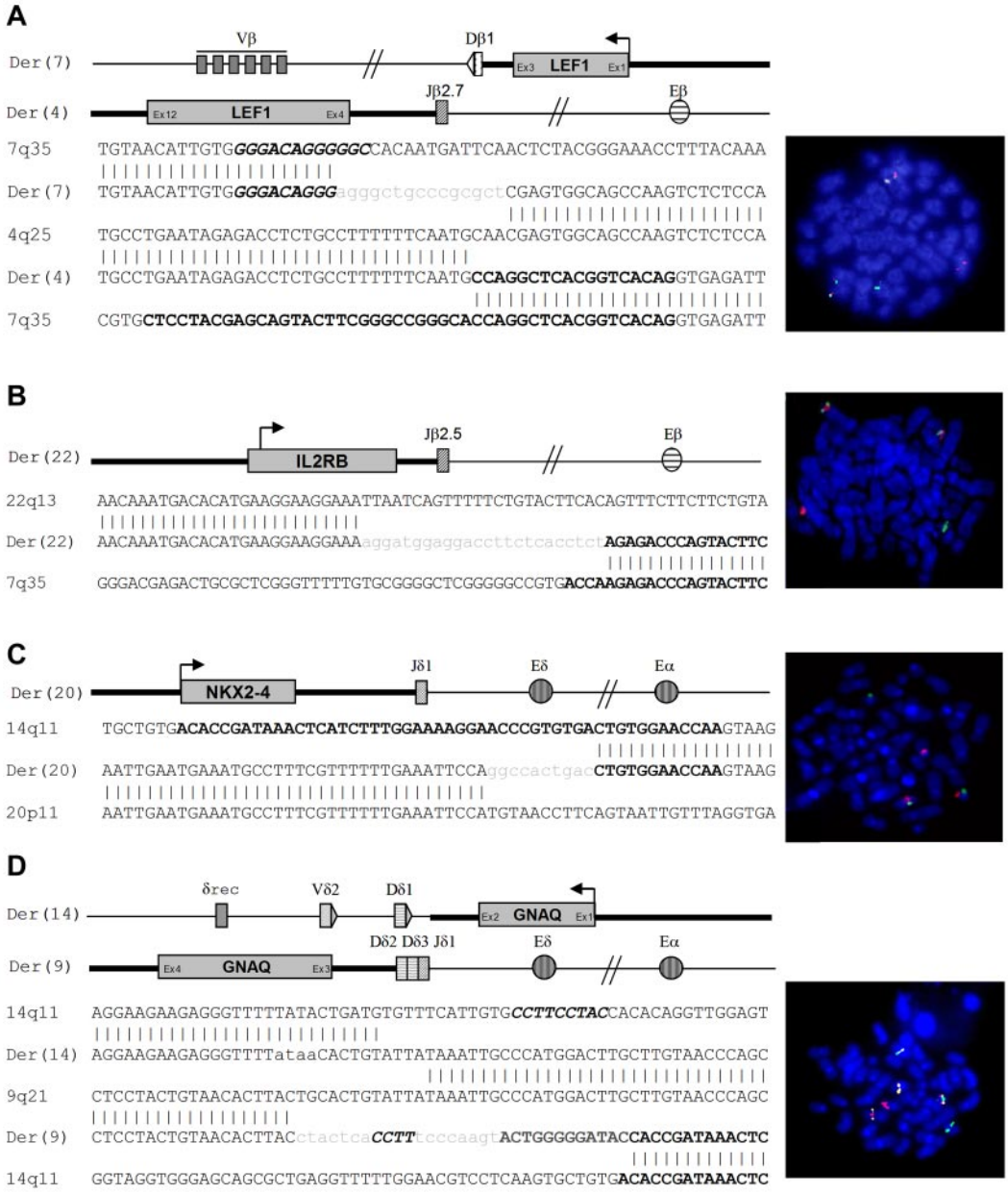

Figure 1. Novel TCR-oncogene translocations with FISH profiles. (A-B) New TCRβ oncogene partner. Bold and thin bars depict the 4q25 or 22q13 and 7q34 chromosomal regions, respectively. Untemplated nucleotides (n diversity) are indicated in lowercase. Nucleotide sequences for the Dβ1, and Jβ gene segments are depicted in italic bold and bold, respectively. Rights panels show a typical FISH metaphase analysis with a normal allele (split spots) and a translocated allele (fused spots) with TCRβ (green) and oncogenes (red) probes. (C) New TCRα/δ oncogene partner. Bold and thin bars depict the 20p11 or 9q21 and 14q11 chromosomal regions, respectively. Untemplated nucleotides (n diversity) are indicated in lowercase. Nucleotide sequences for the Dδ2, Dδ3, and Jδ1 gene segments are depicted in bold italic, dark gray, and bold, respectively. Right panel show a typical FISH analysis on metaphase with a normal allele (split spots) and a translocated allele (fused spots) with TCRα/δ (green) and oncogenes (red) probes. (D) Three-color FISH analysis using a combination of TLX1 (green), GNAQ (yellow), and TCRα/δ (red) probes.

and *TCR*α/δ–translocated patients (Figure 3 and supplemental Figure 6), respectively. All 11 *TCR*β-oncogene T-ALL patients in which both derivative junctions were identified occurred during a Dβ to Jβ rearrangement (Figure 2 and supplemental Figure 5), of which 10 were Dβ1 and 2 were Dβ2. In patient T-ALL536, a Vβ-Dβ rearrangement occurred after translocation. Similarly, the *TCR*α/δ translocated cases predominantly (12 of 15) demonstrated junctions involving Dδ2 or Dδ3 to Jδ1 errors (Figure 3 and supplemental Figure 6). Only 1 patient (T-ALL268) had translocation with TCRα. Therefore, *TCR*α/δ and *TCR*β-oncogene translocations must occur during early thymic-cell differentiation in the majority of both adult and pediatric patients.[23] These data also imply that oncogene activation takes place at an immature DN/CD1a$^-$/CD34$^+$ stage of thymic development, when Dδ2-Dδ3/Dδ3-Jδ1 and Dβ-Jβ rearrangements occur, whereas the bulk of leukemic maturation arrest occurs at a later (cortical) stage. This strongly suggests that most TCR-oncogene translocations correspond to early "driver" events in T-ALL oncogenesis.

Most TCR partner oncogene breakpoints appeared to not be recombinase mediated

Because all TCRβ junctions identified involved DNA transactions between 3 breaks (6 DNA ends type 2), the breaks in the oncogene partner are unlikely to be RSS mediated. This was also the case for the majority of *TCR*α/δ-oncogene junctions. None of the 26 fully

Table 2. Biological characteristics of T-ALL with TCRδ-oncogene translocation

T-ALL UPN	Age, y	Phenotype	Oncogenetic	TCRδ partner	Karyotype
Pediatric T-ALL (n = 9)					
103*	12	IMβ	TLX1	TLX1	46,XY[20]
346*	5	IMβ	TLX1	TLX1	ND
377	15	Pre-αβ	Negative	LMO2	47,XY,del(9)(p?),t(11;14)(p13.q11),+17[22]
169	13	Pre-αβ	Negative	LMO2	46,XY[20]
299	12	Pre-αβ	Negative	LMO2	46,XX[24]
86	14	Pre-αβ	Negative	TAL1	46,XY,inv(2)(p25q21)[22]
327	15	TCRαβ+	Negative	TAL1	ND
268	13	TCRαβ+	Negative	MYC	46,XY,t(8;14)(q24;q11)[18]/46,XY,i(17)(p10)[5]/46,XY[5]
391	7	IMβ	TLX3	IGLV5–45	47,XX,+8,del(9)(p21p24)[24]
Adult T-ALL (n = 29)					
135*	24	IMβ	TLX1	TLX1	48,XY,del(3)(q27),add(4)(q34),+5,+21[9]/48,idem,−17,+mar[2]/46,XY[19]
516*	38	IMβ	TLX1	TLX1	46,XX[30]
506*	35	Pre-αβ	TLX1	TLX1	47,XY,del(6)(q16q24),del(8)(p11),t(10;14)(q24;q11),+mar[6]/46,XY[10]
480*	41	Pre-αβ	TLX1	TLX1	46,XY,del(6)(q13q23),add(9)(p11),t(10;14)(q24,q11)[8]/46,XY[4]
199*	31	Pre-αβ	TLX1	TLX1	ND
281*	18	Pre-αβ	TLX1	TLX1	46,XY[20]
496*	27	Pre-αβ	TLX1	TLX1	46,XY[20]
12*	34	Pre-αβ	TLX1	TLX1	ND
242*	42	Pre-αβ	TLX1	TLX1	46,XY,del(6)(q21q25),t(10;14)(q24;q11)[4]/46,XY[16]
362*	45	Pre-αβ	TLX1	TLX1	46,XY,t(10;14)(q24;q11)[14]/46,XY[4]
9*	48	Pre-αβ	TLX1	TLX1	ND
494*	53	Pre-αβ	TLX1	TLX1	50,idem,+8,t(10;14)(q24;q11),+18,+19,+20[19]
73*	20	Pre-αβ	TLX1	TLX1	46,XY,del(7)(q?),−9,−10,del(12)(p11),−14,−14,+4mar[12]/46,XY[8]
381*	43	Pre-αβ	TLX1	TLX1	46,XY[20]
164*	35	Pre-αβ	TLX1	TLX1	46,XY,t(9;20)(p21;q12),t(10;14)(q24;q11),del(12)(p12)[13]/46,XY[12]
528*	53	TCRγδ+	TLX1	TLX1	ND
499*	21	ND	TLX1	TLX1	46,XY[20]
500	26	Pre-αβ	TLX1	TLX1 and TCRβ	46,XY[20]
244	22	Pre-αβ	TLX1	GNAQ-TLX1	46,XX,t(5;17)(q31;p13),t(9;10;14)(p?;q22;?q23;q11)[20]
260	56	TCRαβ+	Negative	LMO2	ND
437	17	IMγ	Negative	LMO2	46,XY,t(11;14)(p13;q11)[6]/46,XY[12]
481	23	Pre-αβ	Negative	LMO2	46,XY[25]
23	16	Pre-αβ	STIL-TAL1	LMO2	45,XY,−7,del(9)(p21),t(11;14)(p13;q11);[19]
439	25	Pre-αβ	Negative	NKX2–4	46,XY,t(4;7)(q2?5;q35),t(14;20)(q11;p1?2)[19]
145	20	Pre-αβ	Negative	TAL1	ND
486	24	Pre-αβ	Negative	TAL1	46,XY,t(1;14)(p32;q11),del(9)(p?)[18]
92	33	TCRαβ+	Negative	TAL1	45,XY,der(1)t(1;9;14)(p32;p?;q?),der(9)t(1;9;14),−14[3]/47,XY,idem,+2mar[17]/46,XY[4]
45	22	IMβ	STIL-TAL1	Unknown	46,XY,t(5;20)(q32;p13)[3]/46,XY[17]
388	53	Pre-αβ	Negative	Unknown	45,XY,−8,der(8)t(8;?)(q24;?),t(9;14)(p21;q13)[18]

ND indicates not done; and unknown, LM-PCR failures.
*Also reported in Dadi et al.[15]

(both derivatives) characterized TCRα/δ translocations were standard type 1 translocations: trans-V(D)J recombination between 1 TCR RSS and 1 cRSS). Although a heptamer-like sequence located near this hotspot breakpoint region has already been proposed,[24] all *TCR*δ-*TLX1* junctions identified showed the presence of 3 breaks (Dδ, Jδ1, and *TLX1*), suggesting a type 2 translocation. To further test these reported heptamer-like sequences, the whole 700-bp region from 5′ to *TLX1* was tested by a functional extrachromosomal recombination assay (supplemental Figure 7A). Consistent with previous reports,[24] this confirmed the absence of functional cryptic RSS that could drive the *TLX1* break location by this in vitro assay (supplemental Figure 7B). We also used the recently developed RSS Information Content (RIC) score analysis, an in silico tool allowing evaluation of the recombinogenic potential of cRSS candidates (http://www.itb.cnr.it/rss). The RIC scores obtained for the recombination sites involved at all 39 breakpoints showed that the large majority of translocations reported here (37 of 39) do not pass the RIC criteria, confirming the absence of functional cRSS and the status of type 2 translocations. In only 2 cases, T-ALL43 (RIC: −32.86) and T-ALL86 (RIC: −54.19), did a borderline "pass" RIC score identify potential 12-RSS and 23-RSS candidates, respectively (supplemental Figure 7C). However, neither of the 2 cases would represent a standard trans-V(D)J transaction after cRSS mistargeting. Patient T-ALL43 indeed showed a *TLX1* cRSS/Jβ breakpoint with a long N insertion (supplemental Figure 5), which might be compatible with a type 1 translocation followed by rare ongoing recombination of the SJ (leading to a pseudo-HJ[25]). Unfortunately, neither LM-PCR assays nor direct PCR attempts to identify the expected reciprocal *TLX/D*β–coding joint on der(7) gave rise to amplification products, preventing definitive resolution of this case. Patient T-ALL86 was even more complex, and compatible with a rare variant involving the collusion between a type 1 synapse (Dδ2-12/*TAL1*) and a Dδ2-Dδ3 rearrangement.[26]

To explore whether CpG dinucleotides are involved in the type 2 translocations identified herein (as described previously in the *BCL2* MBR, *BCL1* MTC, and the *TCF3* clusters to be hotspots for translocation breakpoints in B-lymphoid lymphomas and leukemias[27]),

Table 3. Immunophenotypic genotypic characteristics and NOTCH1/FBXW7 status of adult T-ALL as a function of TCR translocation

	n	T-ALL TCRβ translocated, n (%)	T-ALL TCRδ translocated, n (%)	T-ALL TCRβ/δ nontranslocated, n (%)
T-ALL patients	280	40 (14%)	38 (13%)	205 (73%)
Median age, y	18	19,5	24	17
TCR subset analysis				
Immature	58	4 (7%)	1 (2%)	53 (91%)
IMβ/pre-αβ	143	26 (18%)	31 (22%)	89 (60%)
TCRγδ	40	7 (18%)	1 (2%)	32 (80%)
TCRαβ	35	3 (9%)	4 (11%)	28 (80%)
ND	4	0	1	3
Genotype subset analysis				
PICALM-MLLT10	18	2 (11%)*	0	16 (89%)
STIL-TAL1	30	2 (7%)†	2 (7%)‡	26 (86%)
TLX1	39	11 (28%)§	21 (54%)§	7 (18%)
TLX3	47	1 (2%)	1 (2%)¶	45 (96%)
None of above	146	22 (15%)	14 (9%)	111 (76%)
NOTCH1 FBXW7 mutation				
NOTCH1 and/or FBXW7 mutated	150	25 (71%)	24 (83%)	101 (63%)
NOTCH1 and FBXW7 unmutated	73	10 (14%)	5 (7%)	61 (84%)
ND	57	5	9	43

ND indicates not done.
*Both TCRβ-HOXA.
†LMO1 and IL2RB.
‡LMO2 and failed.
§All TCR-TLX1.
¶Trans-rearrangement Ig-TCRδ.

we searched for CpG dinucleotides and *TLX1* breakpoint colocalization, but found that they were not superimposed (supplemental Figure 8). This suggested that distinct, as yet unrecognized, mechanisms are responsible for these breaks. Finally, because most of the oncogenic regions did not have cryptic heptamers and TCR-oncogene chromosomal translocations involved DNA transactions between 3 breaks in a large majority of cases, our data suggest that strand donation within type 2 translocations represent the most frequent illegitimate translocation events in T-ALL. However, we cannot formally exclude that some of the cRSS might have taken part in complex nonconventional type 1 translocations, and further studies will be necessary to fully explore the interesting possibility of complex 2-step recombination and/or 3-way synapses.

TCRβ- and TCRα/δ–translocated oncogenes are driven by distinct transcriptional regulators

In TCRβ translocations, the regulatory element that drives oncogene expression is likely to be exclusively Eβ, because the oncogene and the Eβ enhancer were located on the same derivative chromosome in all cases (Figure 2). In contrast, TCRα/δ translocations demonstrated heterogeneity with respect to the relative position of oncogenes and TCR^+ regulatory elements on the derivative chromosomes. A minority (n = 4) were compatible with Eα/δ–driven oncogenesis, all of which involved *MYC*, *LMO2*, or *TAL1* (Figure 3). In all remaining cases (20 of 24), the oncogene and Eα/δ were not on the same derivative chromosome, demonstrating that oncogene overexpression must be because of distinct regulatory elements within the TCRδ locus.

Virtually all of the *TCR*α/δ-*TLX1* breakpoints were within the *TLX1* exon 1 (5′ to the ATG start site and 3′ to the promoter), leading to separation of the *TLX1* promoter from the coding region. To determine the origin of TCR-driven TLX1 transcripts, we performed clono-specific RT-PCR across the breakpoints of both *TCR*α/δ-*TLX1* and *TCR*β-*TLX1* translocations. "Fusion transcripts" (resulting from transcription within the TCRα/δ locus) were detected in all of the *TCR*α/δ-*TLX1* samples (Figure 4A), but not in the *TCR*β-*TLX1* samples (data not shown and as described previously[15]), suggesting the presence of positive regulatory element(s) upstream to the *TCR*δ locus that drives TLX1 overexpression. In contrast, in patients with *TCR*α/δ-*LMO2* or *TCR*α/δ-*TAL1* translocations with the same configuration, no fusion transcripts from the TCRδ locus could be identified (Figure 4B). These data demonstrate that the mechanisms driving oncogene deregulation other than by downstream enhancer juxtapositioning are different in $TLX1^+$ and $TLX1^-$ T-ALL.

The levels of LMO2, TAL1, and TLX1 expression did not differ depending on whether expression was driven by Eβ, Eα, or upstream TCRδ regulatory elements (or cryptic promoters), demonstrating that sufficient levels of transcriptional deregulation are likely to be required for oncogenic clonal selection (Figure 4C). Consistent with this observation, breakpoints were scatted, often at a significant distance from the oncogene, in enhancer-driven (Eβ or Eα) TCR-oncogene cases. In contrast, they clustered close to the oncogene when the oncogene and Eα/δ were located on different derivative chromosomes, in keeping with promoter-dependent, *cis*-acting positive regulatory elements (Figures 2 and 3).

Overall, these data demonstrate that enhancer-independent oncogene deregulation and clonal selection occurs frequently in *TCR*α/δ, but not in *TCR*β translocations in T-ALL.

Discussion

Deciphering the molecular mechanisms of chromosomal alterations in cancer cells has improved our understanding of both the selection of mechanistic pathways and oncogenic functions. Among the various alterations reported to date, TCR chromosome translocations represent the recurrent oncogenic hallmarks of T-ALL,

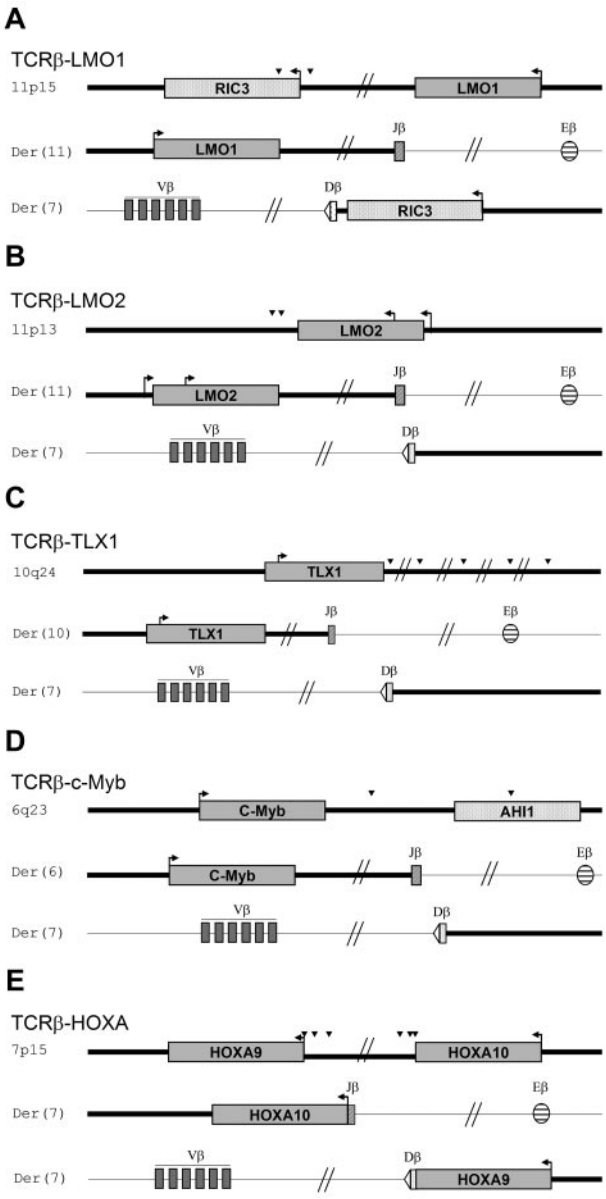

Figure 2. Schematic representation of TCRβ-oncogene translocations. Shown are schematic representations of TCRβ-oncogene translocations: *TCR*β-*LMO1* (A), *TCR*β-*LMO2* (B), *TCR*β-*TLX1* (C), *TCR*β-*MYB* (D), and *TCR*β-*HOXA* (E). Both translocation derivatives are represented. Arrowheads indicate the relative position of breakpoints within the oncogene. Bold and thin bars depict the oncogene locus and the chromosome 7q35 *TCRβ* locus, respectively.

when they are much more frequent than Ig in B-lineage ALL. In the present large series of T-ALL patients analyzed by FISH and/or LM-PCR for *TCR*-oncogene translocation, *TCR*β-oncogene and *TCR*α/δ-oncogene translocations were found in 14% and 13% of T-ALL patients, respectively. A significant number of both *TCR*β and *TCR*α/δ translocations were unsuspected from cytogenetic analysis, stressing the need for FISH/LM-PCR screening if these cases require comprehensive detection. These data are consistent with those of Cauwelier et al, although they reported a slightly higher rate (19%) of *TCR*β-oncogene translocation.[4] Four new TCR partners were identified in the present series of T-ALL patients: *IL2RB* and *LEF1* with *TCRβ* and *NKX2-4* and *GNAQ* with *TCRα/δ*. The *LEF1* chromosomal translocation was associated with an intragenic deletion of the nontranslocated *LEF1* locus. This suggests an intriguing form of oncogenic inactivation by a *TCR* translocation because the breakpoint within the *LEF1* gene splits the β-catenin domain, confirming the probable tumor-suppressor role of LEF1 reported by Gutierrez et al.[21] A translocation involving *IL2RB* has been described with an unknown partner on chromosome 1.[28] IL2RB is constitutively expressed in mature T cells and is induced by TCR activation, leading to proliferation and T-cell survival.[29] An oncogenic role for IL2RB deregulation is not evident because it does not have catalytic properties. Further investigation will be necessary to clarify this uncommon abnormality. A *TCR*α/δ-*NKX2-4* translocation could be suspected from a t(14;20)(q11;p12) karyotype reported by Cauwelier et al.[4] *NKX2-4* is a member of the NKL family of homeodomain proteins, which also contains *TLX1* and *TLX3*.[30] Recently, deregulation of other NKL oncogenes (*NKX2.1*, *NKX2.2*, and *NKX2.5*) were reported in T-ALL.[31,32] Both *NKX2.1* and *NKX2.2* are known to be deregulated by recurrent *IgH/TCR* translocations. However, such translocations are likely to be rare, because none was identified in the present large series. Interestingly, T-ALL with *NKX2.1* overexpression corresponds to a distinctive transcriptional cluster characterized by a proliferative profile. Unfortunately, gene-expression profiling was unavailable for the *NKX2-4* translocated patient reported here. Another NKL member, *NKX2-5*, can be deregulated by juxtapositioning to *BCL11B* in pediatric T-ALL cell lines.[32] These observations suggest that a variety of NKL (at least TLX and NKX) proteins can be involved in T-ALL oncogenic networks. Despite these 4 patients, few novel oncogenes have been identified in the present study, suggesting that the large majority of TCR-driven oncogenes in T-ALL have already been identified.

Mistakes of V(D)J recombination have been considered one of the major mechanisms leading to lymphoid malignancy-associated translocations. Concerning type 2 translocations, the V(D)J synaptic complex is formed between the 2 normal *TCR/IG* partners. In this case, the end transaction corresponds to a mistake in the repair phase of the V(D)J recombination, illegitimately joining coding-end intermediates (D and J) with broken ends (tumor breakpoints) and joining the signal-end intermediates into a normal signal-joint (SJ), which is not seen in tumor cells excised on a nonreplicative episome diluted out during successive cell divisions.[8,33] Because the RAGs can perform a single-strand nick at an isolated RSS (or cRSS), but requires a synaptic complex to convert the nick into a double-strand break,[34] the possibility that a broken end (or any third RSS partner) would have been converted from a nick into a double-strand break before engaging in repair with synapsed partners is slim. No tripartite V(D)J reaction involving 2 *IG/TCR* partners and an additional RSS has been demonstrated so far.

A confusing situation may arise when the type 1 signal joint generated on one of the derivative chromosomes keeps on rearranging with *IG/TCR* partners in *cis*. This may create a pseudo-hybrid joint (ΨHJ) between a *TCR/IG* coding end and the cRSS, but in which both rearranging partners (the coding end and the cRSS) undergo processing (deletion, P, and N regions).[35] Although this 2-step mechanism has to date rarely been reported,[25] we cannot exclude that it might be involved in some of the translocations reported herein. Translocations of type 2 are generally more scattered, but nevertheless can cluster in "fragile sites" (within hundreds of base pairs) near the deregulated oncogene. A recent study tested cRSS in several oncogenes and showed that only few pseudo-RSS support V(D)J recombination in in vitro models, suggesting that V(D)J targeting mistakes are only responsible for a modest fraction of genomic alterations.[7] Our present data are in keeping with these

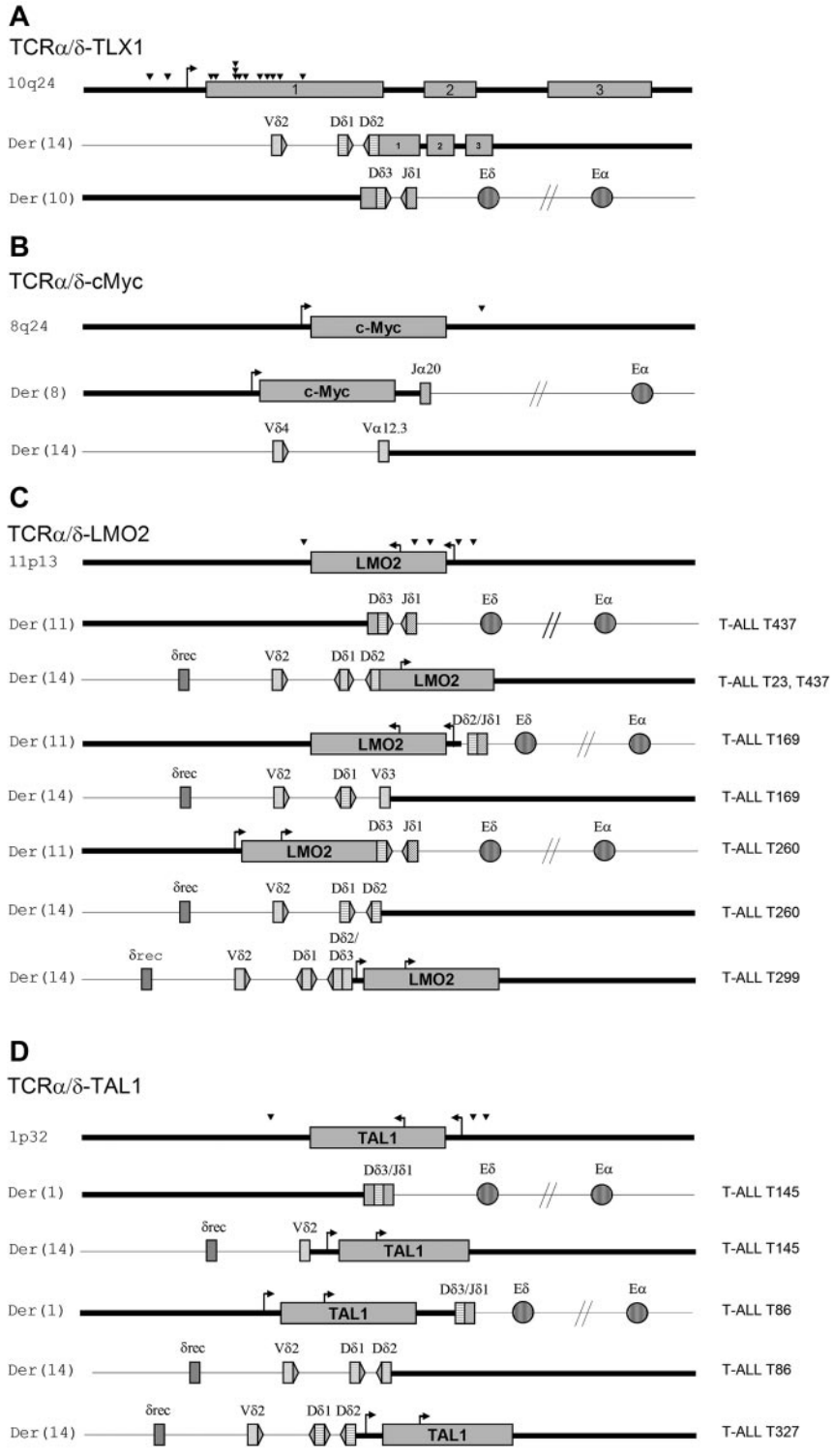

Figure 3. Schematic representation of TCRα/δ-oncogene translocations. (A-D) Shown are schematic representations of TCRα/δ-oncogene translocations: *TCRα/δ-TLX1* (A), *TCRα/δ-MYC* (B), *TCRα/δ-LMO2* (C), and *TCRα/δ-TAL1* (D). Both translocation derivatives are represented, with corresponding T-ALL unique patient numbers. Arrowheads indicate the relative positions of breakpoints within the oncogene. Bold and thin bars depict the oncogene locus and chromosome 14q11 *TCRα/δ,* respectively.

functional studies, because molecular analysis of TCR-oncogene junctions showed a large majority of type 2 TCR-oncogene translocations in which the TCR partner chromosome breakpoints were not RAG mediated. CpG dinucleotides in the *BCL2* MBR, *BCL1* MTC, and *TCF3* breakpoint clusters have been reported to be hot spots for translocation breakpoints,[27] but we found no superimposition of CpG dinucleotides and *TLX1* breakpoints, which are highly clustered (supplemental Figure 8). This suggests that type 2 V(D)J translocations in T-ALL involve non-RAG double-strand break mechanisms distinct from those identified in B-lymphoid malignancies.

The majority of *TCR* translocations occurred during Dβ-Jβ or Dδ-Dδ rearrangements, known to be very early events in T-cell differentiation that occur within the thymus in DN CD1a$^-$ cells before TCRβ selection. The final maturation arrest of the bulk leukemic population was much later in most cases,

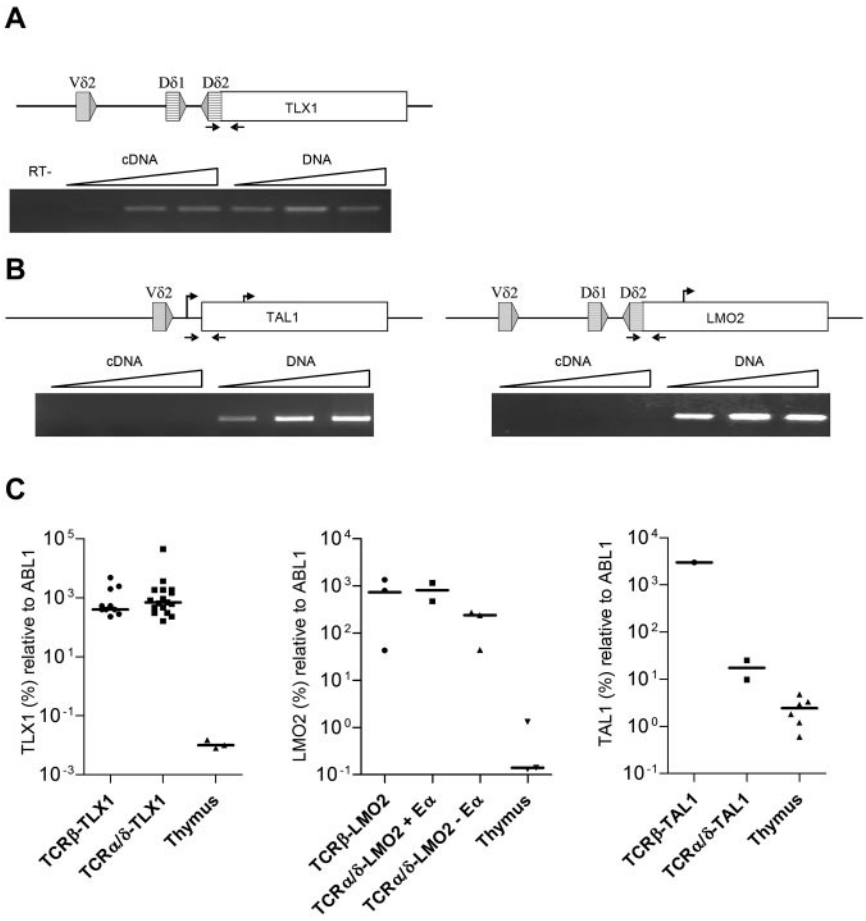

Figure 4. Analysis of the TCR-oncogene translocation. (A) Fusion transcripts from *TCR*δ-*TLX1* (T-ALL9) were investigated by PCR and RT-PCR with a range of cDNA and DNA quantities. (B) *TCR*δ-*LMO2* (T-ALL145) and *TCR*δ-*TAL1* (T-ALL437) translocations were investigated by PCR and RT-PCR with a range of cDNA and DNA quantities (positions of oligonucleotide primers are indicated by arrows on upper diagrams). The absence of genomic DNA contamination in the cDNA fraction was validated by quantitative RT-PCR using albumin DNA-specific oligonucleotide primers (not shown) and a RT-negative control was performed for T-ALL9. (C) *TLX1*, *LMO2*, and *TAL1* quantification by quantitative RT-PCR.

demonstrating uncoupled oncogene activation and maturation arrest. Most TCR-translocated T-ALLs were indeed arrested during or after TCRβ selection, with a significant proportion expressing a TCRαβ or TCRγδ. We demonstrated that a significant proportion of these TCR^+ T-ALLs, especially those expressing a TCRγδ, retain stigmata of TCRβ selection, such as a DP, $CD1a^+$ phenotype and ongoing RAG1 and pre-T-α expression.[12] These data are compatible with an oncogenic role for the pro-proliferative TCRβ selection signal, whereby the *TCR* translocation occurs in an early DN thymocyte, but leads to a maturation arrest around TCRβ selection, as recently described for *TCR*α/δ-*TLX1* translocations.[15] Consistent with this, most *TCR* translocations are associated with specific stages of maturation arrest, the so-called type A oncogenes.[36] The scenario in which oncogene activation is uncoupled from oncogene activity entails that the cell carrying the translocation has no selective advantage until reaching the appropriate later stage, when maturation is arrested. This cell and its progeny will meanwhile accumulate imprints of poly/oligoclonality, such as *TCR* rearrangements and additional oncogenic mutations. Monoclonality would arise through competitive advantage of the additional mutations/translocations (it is currently considered that T-ALLs usually have > 10 mutations/T-ALL) subsequently occurring in one or another subclone. Although this is only beginning to be recognized in T-ALL, this concept has clearly been demonstrated in other lymphoid neoplasms. The best-described example is the t(14;18)–mediated translocation in follicular lymphoma leading to ectopic BCL2 expression. Although the translocation occurs as a type 2 translocation during the DH to JH recombination in the BM, BCL2 does not prevent further B-cell differentiation or provide a selective advantage until reaching the germinal center, the quasi-exclusive localization where BCL2 is physiologically down-regulated.[37,38] As a consequence, follicular lymphoma manifests as a mature B-cell lymphoma originating from the germinal center. Demonstrative evidence that this uncoupling also occurs in T-ALL oncogenesis is the *Notch1* mouse model, in which the retrovirus-mediated overexpression of intracellular notch (ICN1) in Lin^- BM cells generates $TCR\alpha\beta^+CD4^+CD8^+$ T-ALLs with a monoclonal TCRβ chain but diverse TCRα chains.[39] These observations have speculative implications for T-ALL therapy, because the "pre-leukemic" early thymic clonogenic population needs to be eradicated and its disappearance monitored.

A 2-step model of translocation has been proposed based on a *TCR*β-*TAL2* translocation model: (1) a cRSS located 3′ to *TAL2* reacts with Dβ1 in the thymus of a healthy subject and then (2) a Dβ1-Jβ2.7 rearrangement occur, which leads to TAL2 overexpression.[25] This mechanism is not compatible with the majority of *TCR*β translocations described herein, because Dβ1 and Jβ segments are not on the same derivative.

Although all breaks from *TCR*β-oncogene translocations mapped 3′ to the oncogene, the majority of breaks from *TCR*α/δ-oncogene translocations mapped 5′ to the oncogene. Therefore, although oncogene activation in *TCR*β–translocated patients was consistent with classic TCRβ Eβ-mediated activation, the *TCR*α/δ translocations uncoupled the oncogene and Eα

onto 2 distinct derivative chromosomes, implying a distinct deregulation mechanism (involving potential non-enhancer-regulatory elements in the *TCR*δ promoter region). We have demonstrated that TLX1 leads to inhibition of the TCRα enhancer, via an ETS1 interaction,[15] leading to counterselection of translocations that juxtapose *TLX1* and the TCRα enhancer in *cis*. It is therefore possible that the different types of translocations observed for other T-ALL oncogenes are also affected by the consequences of oncogene expression on juxtaposed *TCR* regulatory elements.

Remarkably, despite the obvious contrast in the mechanisms of oncogene activation (see TLX1 or LMO2 in Figure 4C), no significant differences could be observed in oncogene overexpression levels from *TCR*β and *TCR*α/δ translocation configurations. This suggests oncogenic selection of cases with sufficient/optimal expression levels and distinct molecular mechanisms of oncogene activation with respect to the *TCR* locus orientation involved in the translocation rather than the oncogene itself. Further investigation into the molecular mechanisms of early oncogenic deregulation is therefore justified.

In conclusion, the majority of *TCR* structural translocations in T-ALL have now probably been identified, but the mechanisms leading to chromosomal break and misrepair on the partner chromosome remain unidentified. These translocations occur at an earlier stage than bulk maturation arrest and the localization of *TCR*β and *TCR*α/δ breakpoints differ, probably at least in part because of an impact of the deregulated oncogene on the function of the juxtaposed *TCR* regulatory elements.

Acknowledgments

The authors thank all participants in the LALA-94, GRAALL-2003/05, and FRALLE-93/2000 study groups for collecting and providing data and samples and especially Mrs Veronique Lheritier.

Work in the Necker Hematology Department was supported by grants from the Association de Recherche sur le Cancer and the Fondation de France. S.L.N. was supported by a grant from the Association de Recherche sur le Cancer and the Fondation pour la Recherche Medicale. J.B. was supported by the National Cancer Institute of Canada through an award from the Terry Fox Foundation.

Authorship

Contribution: S.L.N., B.N., E.M., and V.A. wrote the manuscript; S.L.N., R.B.A., M.L., J.B., S. Sungalee, D.P.-B., P.V., C.C., L.L., S. Spicuglia, and B.N. performed the experiments and/or analyzed the data; A.P., L.B., I.R.-W., M.-J.G., N.I., H.D., S.R., and J.S. contributed to the sample collection or provided patient data; and V.A. oversaw the conceptual development of the project.

Conflict-of-interest disclosure: The authors declare no competing financial interests.

Correspondence: Vahid Asnafi, Hôpital Necker Enfants Malades, Laboratoire d'hématologie, 149 rue de Sèvres, 75015 Paris, France; e-mail: vahid.asnafi@nck.aphp.fr.

References

1. Asnafi V, Beldjord K, Boulanger E, et al. Analysis of TCR, pT alpha, and RAG-1 in T-acute lymphoblastic leukemias improves understanding of early human T-lymphoid lineage commitment. *Blood.* 2003;101(7):2693-2703.
2. Ferrando AA, Neuberg DS, Staunton J, et al. Gene expression signatures define novel oncogenic pathways in T cell acute lymphoblastic leukemia. *Cancer Cell.* 2002;1(1):75-87.
3. Aifantis I, Raetz E, Buonamici S. Molecular pathogenesis of T-cell leukaemia and lymphoma. *Nat Rev Immunol.* 2008;8(5):380-390.
4. Cauwelier B, Dastugue N, Cools J, et al. Molecular cytogenetic study of 126 unselected T-ALL cases reveals high incidence of TCRbeta locus rearrangements and putative new T-cell oncogenes. *Leukemia.* 2006;20(7):1238-1244.
5. Arai Y, Hatano M, Tokuhisa T. A negative regulatory region of the murine Hox11 gene. *Gene.* 1997;193(1):73-79.
6. Brake RL, Kees UR, Watt PM. Multiple negative elements contribute to repression of the HOX11 proto-oncogene. *Oncogene.* 1998;17(14):1787-1795.
7. Vanura K, Vrsalovic MM, Le T, et al. V(D)J targeting mistakes occur at low frequency in acute lymphoblastic leukemia. *Genes Chromosomes Cancer.* 2009;48(8):725-736.
8. Marculescu R, Vanura K, Montpellier B, et al. Recombinase, chromosomal translocations and lymphoid neoplasia: targeting mistakes and repair failures. *DNA Repair (Amst).* 2006;5(9-10):1246-1258.
9. Spits H. Development of alphabeta T cells in the human thymus. *Nat Rev Immunol.* 2002;2(10):760-772.
10. Spits H, Blom B, Jaleco AC, et al. Early stages in the development of human T, natural killer and thymic dendritic cells. *Immunol Rev.* 1998;165:75-86.
11. Dik WA, Brahim W, Braun C, et al. CALM-AF10+ T-ALL expression profiles are characterized by overexpression of HOXA and BMI1 oncogenes. *Leukemia.* 2005;19(11):1948-1957.
12. Asnafi V, Radford-Weiss I, Dastugue N, et al. CALM-AF10 is a common fusion transcript in T-ALL and is specific to the TCRgammadelta lineage. *Blood.* 2003;102(3):1000-1006.
13. Armstrong SA, Look AT. Molecular genetics of acute lymphoblastic leukemia. *J Clin Oncol.* 2005;23(26):6306-6315.
14. Graux C, Cools J, Michaux L, Vandenberghe P, Hagemeijer A. Cytogenetics and molecular genetics of T-cell acute lymphoblastic leukemia: from thymocyte to lymphoblast. *Leukemia.* 2006;20(9):1496-1510.
15. Dadi S, Le Noir S, Payet-Bornet D, et al. TLX Homeodomain oncogenes mediate T cell maturation arrest in T-ALL via interaction with ETS1 and suppression of TCRalpha gene expression. *Cancer Cell.* 2012;21(4):563-576.
16. Asnafi V, Beldjord K, Libura M, et al. Age-related phenotypic and oncogenic differences in T-cell acute lymphoblastic leukemias may reflect thymic atrophy. *Blood.* 2004;104(13):4173-4180.
17. Bergeron J, Clappier E, Radford I, et al. Prognostic and oncogenic relevance of TLX1/HOX11 expression level in T-ALLs. *Blood.* 2007;110(7):2324-2330.
18. Przybylski GK, Dik WA, Wanzeck J, et al. Disruption of the BCL11B gene through inv(14)(q11.2q32.31) results in the expression of BCL11B-TRDC fusion transcripts and is associated with the absence of wild-type BCL11B transcripts in T-ALL. *Leukemia.* 2005;19(2):201-208.
19. Marculescu R, Le T, Simon P, Jaeger U, Nadel B. V(D)J-mediated translocations in lymphoid neoplasms: a functional assessment of genomic instability by cryptic sites. *J Exp Med.* 2002;195(1):85-98.
20. Ferrando A, Neuberg D, Dodge RK, et al. Adult T-cell ALL patients whose lymphoblasts express the HOX11 oncogene have an excellent prognosis when treated with chemotherapy and are not candidates for allogeneic bone marrow transplantation in first remission [abstract]. *Blood (ASH Annual Meeting Abstracts).* 2002;100(11):154.
21. Gutierrez A, Sanda T, Ma W, et al. Inactivation of LEF1 in T-cell acute lymphoblastic leukemia. *Blood.* 2010;115(14):2845-2851.
22. Bergeron J, Clappier E, Cauwelier B, et al. HOXA cluster deregulation in T-ALL associated with both a TCRD-HOXA and a CALM-AF10 chromosomal translocation. *Leukemia.* 2006;20(6):1184-1187.
23. Dik WA, Pike-Overzet K, Weerkamp F, et al. New insights on human T cell development by quantitative T cell receptor gene rearrangement studies and gene expression profiling. *J Exp Med.* 2005;201(11):1715-1723.
24. Raghavan SC, Kirsch IR, Lieber MR. Analysis of the V(D)J recombination efficiency at lymphoid chromosomal translocation breakpoints. *J Biol Chem.* 2001;276(31):29126-29133.
25. Marculescu R, Vanura K, Le T, Simon P, Jager U, Nadel B. Distinct t(7;9)(q34;q32) breakpoints in healthy individuals and individuals with T-ALL. *Nat Genet.* 2003;33(3):342-344.
26. Tycko B, Sklar J. Chromosomal translocations in lymphoid neoplasia: a reappraisal of the recombinase model. *Cancer Cells.* 1990;2(1):1-8.
27. Tsai AG, Lu H, Raghavan SC, Muschen M, Hsieh CL, Lieber MR. Human chromosomal translocations at CpG sites and a theoretical basis for their lineage and stage specificity. *Cell.* 2008;135(6):1130-1142.

28. Berger R, Bernard OA. Interleukin-2 receptor beta chain locus rearrangement in a T-cell acute lymphoblastic leukemia. *Pathol Biol (Paris)*. 2007; 55(1):56-58.

29. Taniguchi T, Minami Y. The IL-2/IL-2 receptor system: a current overview. *Cell*. 1993;73(1):5-8.

30. Holland PW, Booth HA, Bruford EA. Classification and nomenclature of all human homeobox genes. *BMC Biol*. 2007;5:47.

31. Homminga I, Pieters R, Langerak AW, et al. Integrated transcript and genome analyses reveal NKX2-1 and MEF2C as potential oncogenes in T cell acute lymphoblastic leukemia. *Cancer Cell*. 2011;19(4):484-497.

32. Nagel S, Kaufmann M, Drexler HG, MacLeod RA. The cardiac homeobox gene NKX2-5 is deregulated by juxtaposition with BCL11B in pediatric T-ALL cell lines via a novel t(5;14)(q35.1;q32.2). *Cancer Res*. 2003;63(17):5329-5334.

33. Brandt VL, Roth DB. V(D)J recombination: how to tame a transposase. *Immunol Rev*. 2004;200: 249-260.

34. Roth DB. Restraining the V(D)J recombinase. *Nat Rev Immunol*. 2003;3(8):656-666.

35. Vanura K, Montpellier B, Le T, et al. In vivo reinsertion of excised episomes by the V(D)J recombinase: a potential threat to genomic stability. *PLoS Biol*. 2007;5(3):e43.

36. Van Vlierberghe P, Pieters R, Beverloo HB, Meijerink JP. Molecular-genetic insights in paediatric T-cell acute lymphoblastic leukaemia. *Br J Haematol*. 2008;143(2):153-168.

37. Küppers R. Mechanisms of B-cell lymphoma pathogenesis. *Nat Rev Cancer*. 2005;5(4):251-262.

38. Roulland S, Faroudi M, Mamessier E, Sungalee S, Salles G, Nadel B. Early steps of follicular lymphoma pathogenesis. *Adv Immunol*. 2011;111:1-46.

39. Li X, Gounari F, Protopopov A, Khazaie K, von Boehmer H. Oncogenesis of T-ALL and nonmalignant consequences of overexpressing intracellular NOTCH1. *J Exp Med*. 2008;205(12):2851-2861.

40. Soulier J, Clappier E, Cayuela JM, et al. HOXA genes are included in genetic and biologic networks defining human acute T-cell leukemia (T-ALL). *Blood*. 2005;106(1):274-286.

41. Clappier E, Cuccuini W, Kalota A, et al. The C-MYB locus is involved in chromosomal translocation and genomic duplications in human T-cell acute leukemia (T-ALL), the translocation defining a new T-ALL subtype in very young children. *Blood*. 2007;110(4):1251-1261.